ASIAN JOURNAL OF CIVIL ENGINEERING (BUILDING AND HOUSING) VOL. 11, NO. 3 (2010)
PAGES 397-410

STRENGTH AND BEHAVIOUR OF EXTERIOR BEAM COLUMN JOINTS WITH DIAGONAL CROSS BRACING BARS

K.R. Bindhu[*a] and K.P. Jaya[b]
[a]Department of Civil Engineering, College of Engineering, Thiruvananthapuram, India
[b]Structural Engineering Division, Anna University, Chennai, India

ABSTRACT

The present work aims to study the seismic performance of exterior beam column joint with non-conventional reinforcement detailing. Four joint sub assemblages were tested under reverse cyclic loading applied at beam end. The specimens were sorted into two groups based on the joint reinforcement detailing. The first group (Group A) comprises of two joint assemblages having joint detailing as per construction code of practice in India (IS 456:2000) with two axial load cases. The second group (Group B) comprises of two specimens having additional cross bracing reinforcements for the joints detailed as per IS 456:2000 with similar axial load cases that in first group. The experimental investigations are validated with the analytical studies carried out by finite element models using ANSYS. The experimental results and analytical study indicate that additional cross bracing reinforcements improves the seismic performance.

Keywords: Beam column joint; cyclic load; ductility; finite element models; reinforced concrete; seismic loading

1. INTRODUCTION

Reinforced concrete structures built in zones of low- to-medium seismicity still do not take seismic effect into consideration. The reinforcement details of such structures though conform to the general construction code of practice may not adhere to the modern seismic provisions. Structural engineers often consider current seismic code details for reinforced concrete framed structures impractical. A beam column joint becomes structurally less efficient when subject to large lateral loads, such as strong wind, earthquake, or explosion. In these areas, high percentages of transverse hoops in the core of joints are needed in order to meet the requirement of strength, stiffness and ductility under cyclic loading. Provisions of high percentage of hoops cause congestion of steel leading to construction difficulties.

The performance of beam column joint under seismic conditions has been a research topic for many years. Number of experiments and analytical studies were reported in the

[*] E-mail address of the corresponding author: bindhukr@yahoo.co.in (K.R. Bindhu)

literature. Paulay [1] used the laws of statics and postulated that joint shear reinforcement is necessary to sustain the diagonal compression field rather than to provide confinement to compressed concrete in a joint core. Tsonos et al [2] suggested that the use of crossed inclined bars in the joint region is one of the most effective ways to improve the seismic resistance of exterior reinforced concrete beam-column joints. Murty et al [3] have tested the exterior beam column joint subject to static cyclic loading by changing the anchorage detailing of beam reinforcement and shear reinforcement. The authors reported that the practical joint detailing using hairpin-type reinforcement is a competitive alternative to closed ties in the joint region. Jing et al [4] conducted experiment on interior joints by changing the beam reinforcement detailing pattern at the joint core. Diagonal steel bars in the form of "obtuse Z" were installed in two opposite direction of the joint. The authors found that the non-conventional pattern of reinforcement provided was suitable for joints in regions of low to moderate seismicity. Shyh-Jiann et al [5] investigated the effect of joint hoops on the shear strength of exterior beam-column joint. The authors found that the major function of joint hoop is to carry shear as tension tie and to constrain the width of tension crack. They suggested that lesser amount of joint hoop with wider spacing could be used without affecting the performance of the joint. Alva et al [6] tested four exterior beam-column joints under reversed cyclic loading. The variables were the joint transverse reinforcement and concrete compressive strength. The authors have concluded that concrete compressive strength was the major factor that governs the joint shear capacity. They also found that increasing the number of stirrups increases the joint shear capacity. Elyasian et al [7] studied the response of beams strengthened in shear by fibre-reinforced polymer using ANSYS finite element program. The authors validated the analytical models using available test results from literature and have conducted parametric studies with the model.

The anchorage length requirements for beam bars, the provision of transverse reinforcement and the role of stirrups in shear transfer at the joint are the main issues found from the literatures reviewed. A study of the usage of additional cross-inclined bars at the joint core [2] shows that the inclined bars introduce an additional new mechanism of shear transfer and diagonal cleavage fracture at joint will be avoided. However, there were only limited experimental and analytical studies for the usage of non-conventional detailing of exterior joints. In spite of the wide accumulation of test data, the influence of cross inclined bars on shear strength of joint has not been mentioned in major international codes. In this work an attempt has been made to improve the confinement of core concrete without congestion of reinforcement in joints. The performance of exterior joint assemblages designed for earthquake loads as per IS 1893:2002 [8] and detailed as per current Indian construction code of practice IS 456:2000 [9] are compared with the specimens having additional cross bracing bars provided on two faces of joint as confining reinforcements. The experimental results are validated with the analytical model developed using finite element software package ANSYS.

2. TESTING PROGRAM

The specimens were classified into two groups with two numbers in each group. The group

A specimens were cast with reinforcement detailing as per IS 456: 2000 and using the detailing provisions in SP: 34 [10]. The group B specimens were detailed as per IS 456: 2000 with additional diagonal cross bracing reinforcement at the two faces of the joints for confinement of joint.

2.1 Details of Specimens

All the four beam column joints had identical beam and column sizes. The beams were 150mm deep by 100 mm wide and columns were 150 mm deep by 100 mm wide. The units were one-third of full scale with 550 mm long beams measured from column face with an inter-storey height of 1000 mm. Figure 1 shows the cross section and reinforcement configurations for the specimens. Ordinary Portland cement (53 grade), sand passing through 4.75 mm IS sieve and crushed granite stone of maximum size not exceeding 8 mm were used for the concrete mix. The 28-day compressive strength of the concrete cube was 44.22N/mm^2. Steel bars of yield stress 432N/mm^2 were used as main reinforcement and stirrup. The cover for the longitudinal bars was maintained at 15mm for all the units. Adequate development lengths as per the code requirement were given for the beam longitudinal bars and cross bracing bars to take care of the pull out force. The specimens were cast in horizontal position inside a steel mould. All the specimens were tested under constant axial load and cyclic loading at the end of the beam. One of the specimens from each group was subject to an axial load of 3% of column axial load capacity and the second specimen was subjected to the axial load of 10% of column axial load capacity.

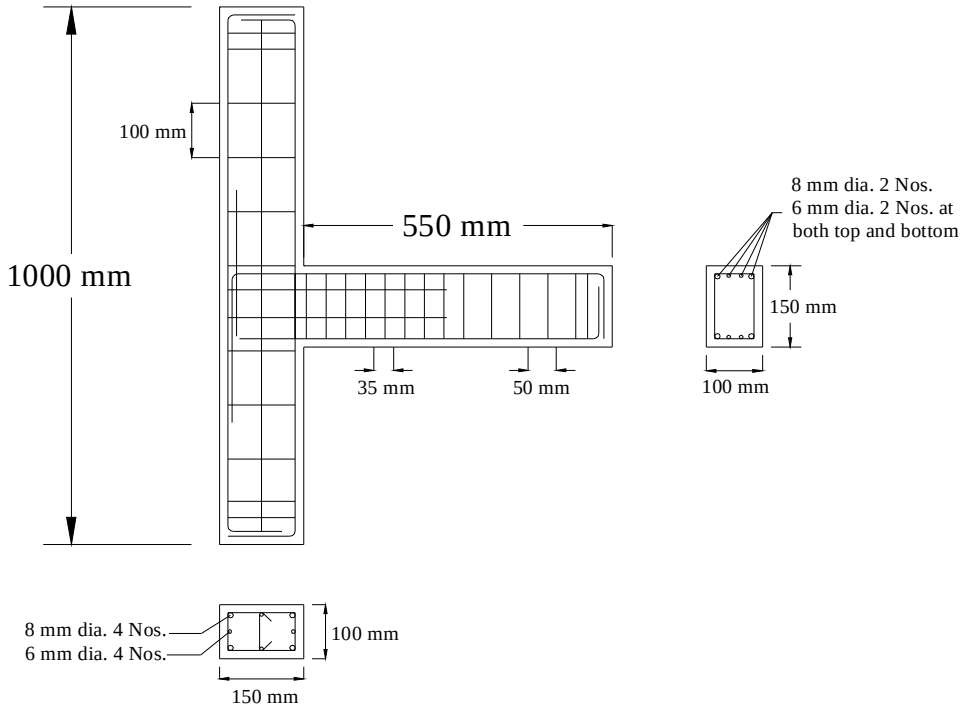

(a) Group A

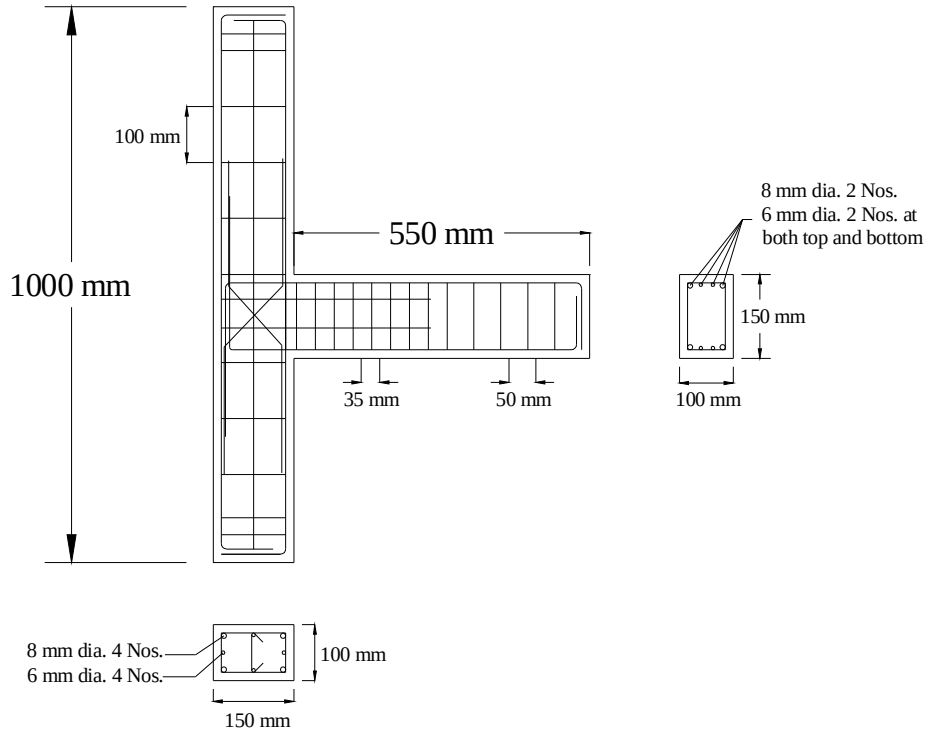

(b) Group B

Figure 1. Reinforcement details of the specimens (a) Group A (As per IS: 456-2000) (b) Group B (As per IS: 456-2000 with non-conventional reinforcement)

2.2 Experimental Program

The schematic view of the test set up is shown in Figure 2. The joint assemblages were subject to axial load and reverse cyclic loading. A constant column axial load was applied by means of a 392.4 kN hydraulic jack mounted vertically to the loading frame for simulating the gravity load on the column. Axial load for the first series specimen was 15.92kN and for the second series was 53.06kN. One end of the column was given an external hinge support, which was fastened to the strong reaction floor, and the other end was laterally restrained by a roller support. Reverse cyclic loading was applied by two 200kN hydraulic jacks, one fixed to the loading frame at the top and other to the strong reaction floor. The point of application of the cyclic load was at 50 mm from the free end of the beam portion of assemblage. The test was load controlled and the specimen was subject to an increasing cyclic load up to failure. The load increment chosen was 1.962kN. Figure 3 shows the loading sequence of the test assemblages. To record loads precisely, load cells having least count 0.0981 kN were used. The specimens were instrumented with Linear Variable Differential Transformer (LVDT) having least count 0.1mm to measure the deflection at loading point.

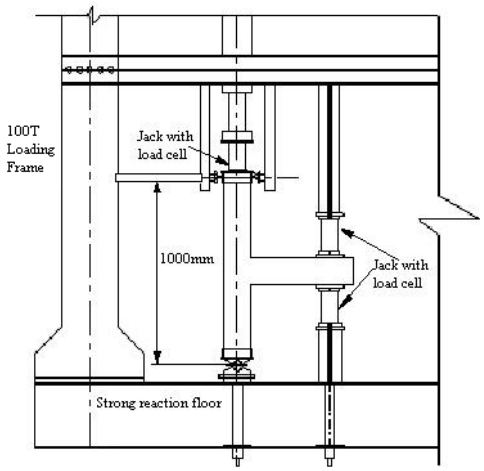

Figure 2. Schematic diagram of test set-up

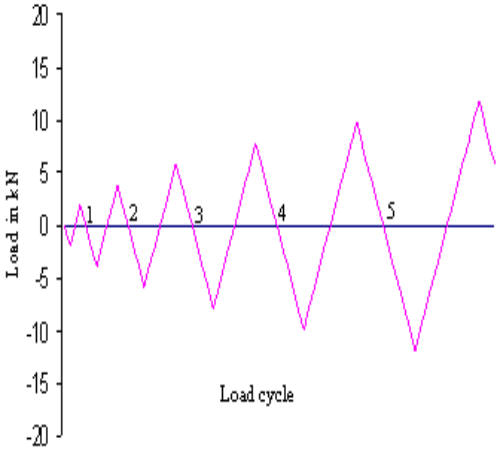

Figure 3. Sequence of cyclic loading

3. ANALYTICAL MODELING

The numerical model represents only half of the beam column joint through width used in the experimental investigation. The symmetry boundary conditions are used in order to simulate the tested joint sub assemblages adequately. The beam column joint was modeled in ANSYS 10 [11] with Solid 65, Solid 45 and Link8 elements. The Solid 65 element was used to model the concrete and Solid 45 element was used to model hinge support at base. These elements have eight nodes with three degrees of freedom at each node- translations in the nodal x, y and z directions. The Link8 element was used to model the reinforcement. This three- dimensional spar element has two nodes with three degrees of freedom at each node – translations in the nodal x, y and z directions.

3.1 Sectional Properties (Real Constants)

The real constants considered for Solid 65 element were volume ratio and orientation angles. Since there was no smeared reinforcement, the real constants (volume ratio and orientation angle) were set to zero. No real constant sets exist for Solid 45 element. The real constants considered for Link8 element are cross sectional area and initial strain.

3.2 Material Properties

The material properties used in the model are given in Table 1. The average 28-day cube strength (f_{cu}) of test specimens was 44.22 MPa. The relationship of cylinder strength ($f_c^{'}$) and cube strength (f_{cu}) given by the ACI Code [12] as ($f_c^{'}$=0.8 f_{cu}) and thus the ultimate compressive strength (f_c') was 35.376 MPa. The uniaxial tensile cracking stress of concrete (f_t) is determined using Equation (1).

$$f_t = 0.623\sqrt{f_c'} \tag{1}$$

The yield stress and tangent modulus of reinforcement bars were obtained from laboratory test. The uniaxial stress-strain relationship for concrete developed by Desayi and Krishnan [13], which is given by Equation (2), was adopted for modeling concrete.

$$f = \frac{E\,\varepsilon}{1+\left(\frac{\varepsilon}{\varepsilon_0}\right)^2} \tag{2}$$

Where,

f = stress at any strain ε

ε_0 = strain at the ultimate compressive strength f_c'

E = a constant (same as initial tangent modulus) such that $E = \frac{2f_c'}{\varepsilon_0}$

Table 1. Material properties defined in model

Material model No.	Element type	Material properties	
1	Link-Spar8	Linear Isotropic	
		EX	$2.1\text{x}10^{11}\text{N/m}^2$
		PRXY	0.3
		Bilinear Kinematic	
		Yield stress	$432\text{x}10^{6}\text{N/m}^2$
		Tangent Modulus	$847\text{x}10^{6}\text{N/m}^2$
2	Solid-Concrete65	Linear Isotropic	
		EX	$3.252\text{x}10^{10}\text{N/m}^2$
		PRXY	0.15
		Concrete	
		Shear transfer coefficient for open crack	0.2
		Shear transfer coefficient for closed crack	0.9
		Uniaxial tensile cracking stress	$3.71\text{x}10^{6}\text{N/m}^2$
3	Solid 45	Linear Isotropic	
		EX	$2.1 \text{ x } 10^{11} \text{ N/m}^2$
		PRXY	0.3

3.3 Modeling of Beam-Column Joint

The beam-column joint is modeled in ANSYS10 software using the above element types and the material properties. Only half of the system was modeled through the thickness so that the symmetry conditions were used. Some of the modeling details are shown in the Figure 4. The axial load is applied on the top of the column with hinged base and a roller support at 50 mm from the top. The load on the beam is applied at a distance of 50 mm from the free end. The models were analyzed with monotonic loadings in the upward and downward direction.

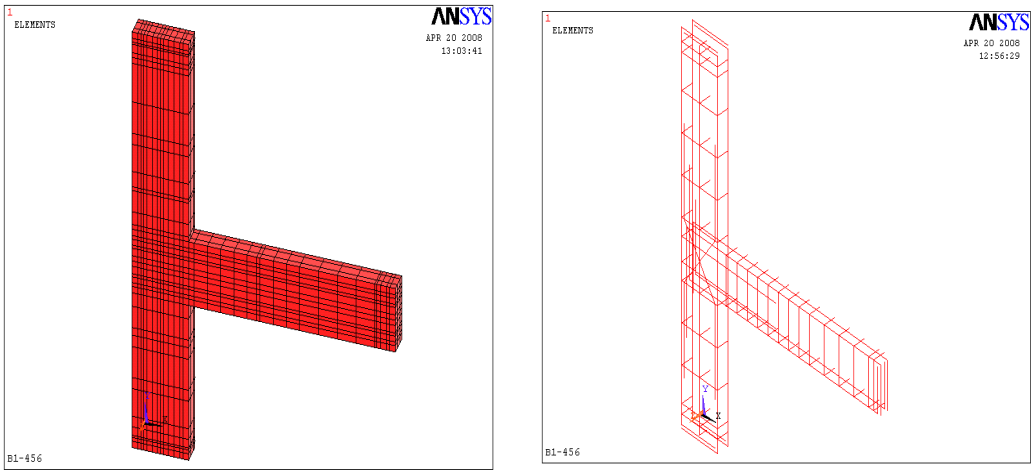

Mesh of concrete and steel support Reinforcement configuration in group B

Figure 4. Modeling details in ANSYS

4. RESULTS AND DISCUSSION

In this section the observations during testing and the results of analytical studies are briefly described.

4.1 Cracking pattern and failure mode of test specimens

The yield and ultimate load for the test specimens are shown in Table 2. The cracking patterns of test specimens in the first and second series of specimens are shown in Figure 5 and Figure 6. In almost all specimens tensile cracks were developed at the interface between the column and beam. A clear vertical cleavage was formed at the junction of all the specimens. For the specimens with diagonal confining bars, no cracks were noticed at the joint and the joint remained intact throughout the test (B1-456 and B2-456). For specimen B2-456 the crack width is also less compared to other specimens.

Table 2. Yield load and ultimate load of specimens from experiment

Designation of specimen	Experimental yield load (kN)			Experimental ultimate load (kN)		
	Downward direction	Upward direction	Average (P_{ye})	Downward direction	Upward direction	Average (P_{ue})
A1-456	13.73	13.73	13.73	15.69	14.71	15.2
B1-456	13.73	13.73	13.73	19.62	19.62	19.62
A2-456	15.7	13.73	14.72	18.64	18.64	18.64
B2-456	15.7	13.73	14.72	19.62	19.62	19.62

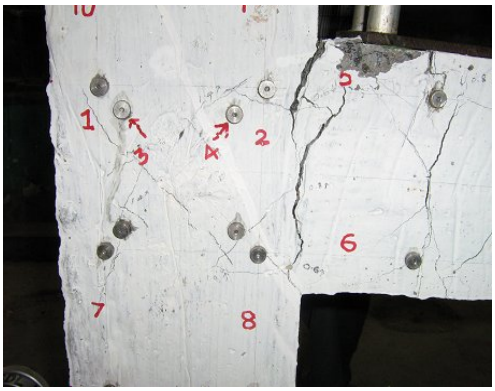

Figure 5(a). Cracks in specimen A1-456

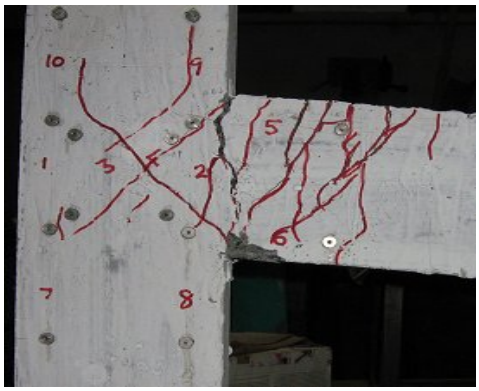

Figure 5(b). Cracks in specimen A2-456

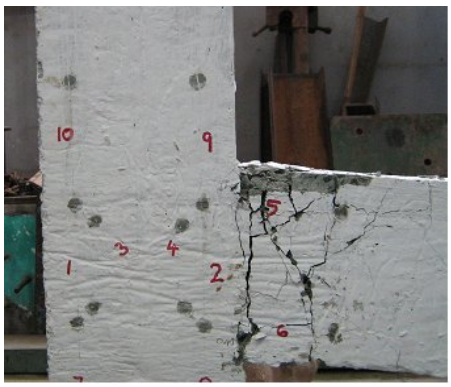

Figure 6(a). Cracks in specimen B1-456

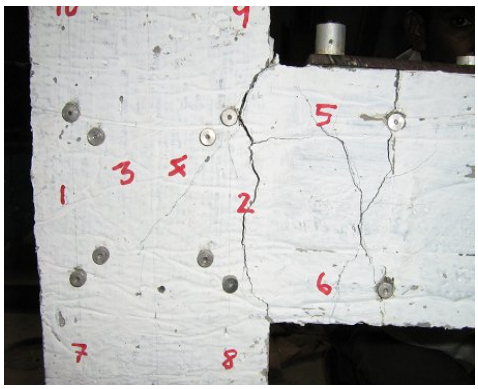

Figure 6(b). Cracks in specimen B2-456

4.2 Hysteretic loops

The force-displacement hysteretic loops for all specimens are as shown in Figure 7 to Figure 10. For the specimens in group B, spindle-shaped hysteresis loops were observed with large energy dissipation capacity. From Table 2 it can be observed that the ultimate load carrying capacity is higher for the specimens in group B. Here the ductility is increased without compromising the stiffness. In general, specimens with diagonal confining bars perform better than conventionally detailed counterparts.

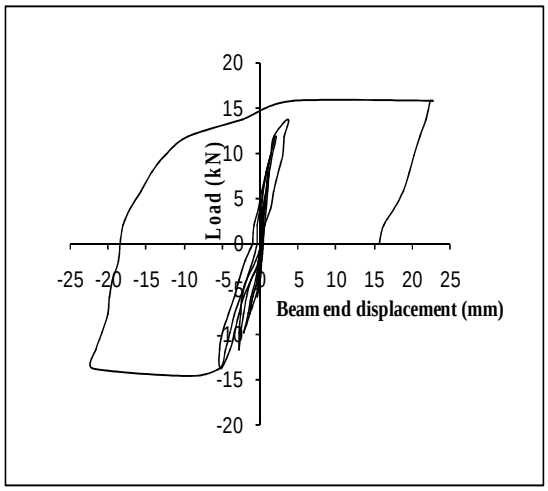

Figure 7. Load-displacement curve of A1-456

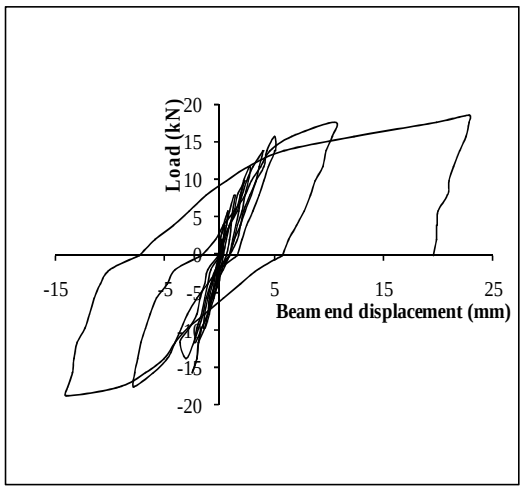

Figure 8. Load-displacement curve of A2-456

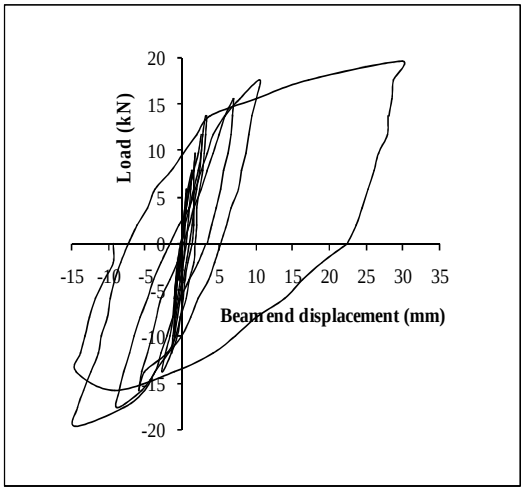

Figure 9. Load-displacement curve of B1-456

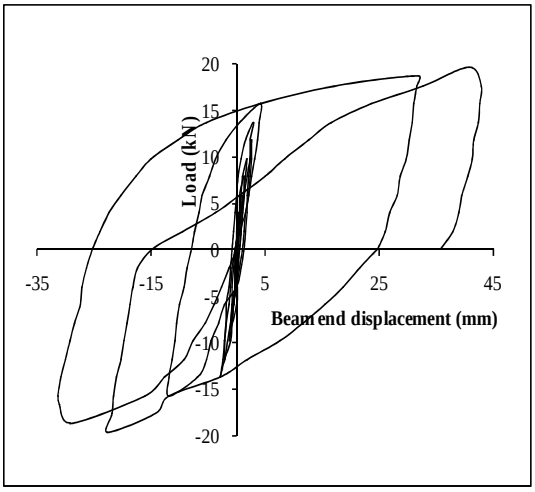

Figure 10. Load-displacement curve of B2-456

4.3 Energy dissipation

The area enclosed by a hysteretic loop at a given cycle represents the energy dissipated by the specimen during that cycle. Comparison of cumulative energy dissipated among the specimens is shown in Figure 11. It is found that the energy dissipation capacity is improved by the addition of diagonal confining bars. For the non-conventionally detailed joints, the axial load is beneficial to dissipate energy.

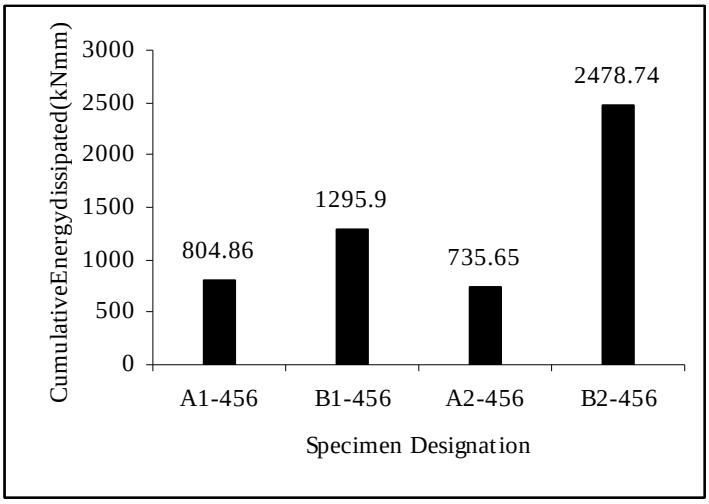

Figure 11. Comparison of cumulative energy dissipated

4.4 Ductility

Ductility is generally measured in terms of displacement ductility, which is the ratio of the maximum deformation that a structure or an element can undergo without significant loss of initial yielding resistance to the initial yield deformation. The displacement ductility for all specimens is presented in Table 3. It is observed that the ductility for the group B specimens have an increase of 14.97% and 114.76% over the corresponding group A specimens. Thus the non-conventional confining reinforcement at joint region improves the ductility of joint. It is observed that the ductility of the joint increases with the increase in the axial load for the specimens in group B, but for the specimens in group A increase in the axial load reduces the ductility.

4.5 Discussion of Analytical study

Load-displacement relationships for monotonic loading in the finite element model of specimens in Group A and Group B are shown in Figure 12(a) through Figure 12(d). The analytical results are compared with the backbone envelope curve of hysteresis loops of load-displacement from the experiment. In general the analytical load-displacement curves agree quite well with the experimental data.

Table 3. Displacement ductility of specimens from experiment

Specimen	Displacement (mm)				Displacement ductility		Average displacement ductility
	Yield		Ultimate				
	Downward direction	Upward direction	Downward direction	Upward direction	Downward direction	Upward direction	
A1-456	3.6	5.3	22.3	22.1	6.19	4.16	6.28
B1-456	3.3	2.7	29.9	14.5	9.06	5.37	7.22
A2-456	5	3	22.8	14	4.56	4.66	4.61
B2-456	4.2	2.9	40.8	29.3	9.71	10.1	9.90

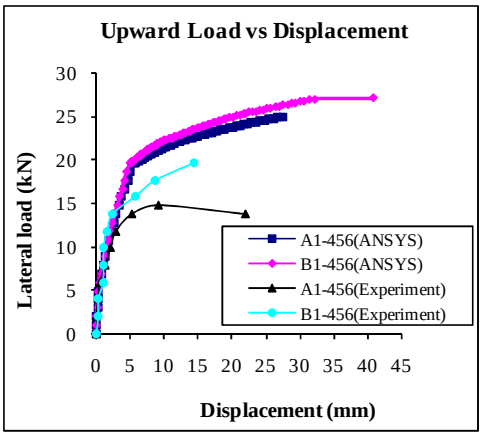

(a). Upward load-displacement curves of joints in first series

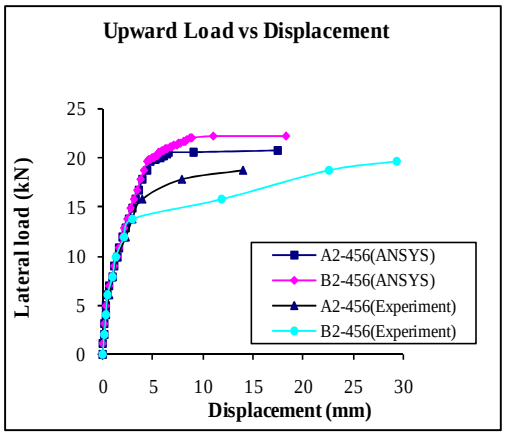

(b). Upward load-displacement curves of joints in second series

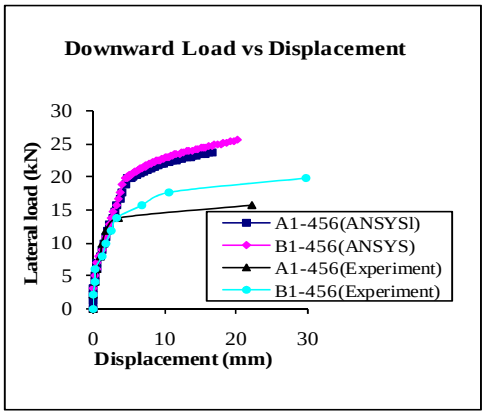

(c). Downward load-displacement curves of joints in first series

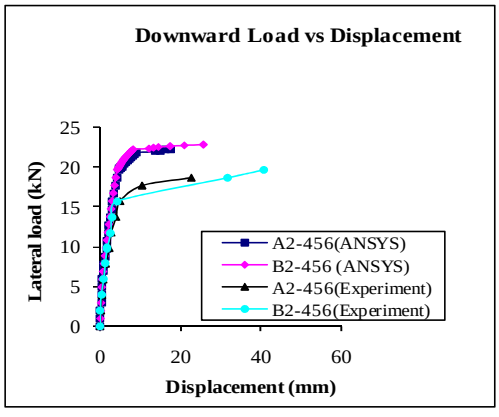

(d). Downward load-displacement curves of joints in second series

Figure 12. Comparison of load-displacement relations of models and specimens

The first cracking load for the finite element analysis are 4.91 kN for the first series specimens (A1-456 and B1-456, for both upward and downward loading) which are higher than the load of 3.92 kN from the experimental results by 25.26%. But for the second series specimens (A2-456 and B2-456), the initial cracks are developed at a load of 5.89 kN which are same as that from the experimental results (5.89 kN). After the first cracking, the finite element models are found stiffer than the tested specimens. The yield load for the first series specimens (A1-456 and B1-456) are 19.71 kN which is higher than the experimental results by 46%. Similarly for the second series, the analytical yield loads are 19.72 kN which is higher than the experimental yield load by 34.06%. The ultimate load carrying capacities of the four models subject to monotonic loading are compared in the Figures 13(a) and 13(b). It is observed that the load carrying capacities are improved in B1-456 and B2-456 compared to A1-456 and A2-456.The final loads from the analytical models in upward loading are 24.92 kN, 27.08 kN, 20.6 kN and 22.17 kN which are higher than the corresponding experimental loads, 14.71 kN, 19.62 kN, 18.64 kN and 19.62 kN by 69.4%, 38.02%, 10.5% and 13% respectively. Similarly the increases in the downward loading are by 50.61%, 29.51%, 19.42% and16%. These higher stiffness in finite element models may be due to the non consideration of the micro cracks in concrete and bond slip of the reinforcement. Thus considering the ultimate load carrying capacities from experimental and analytical studies, the specimens with diagonal confining bars performed well for both the cases of column axial loads. The displacement ductility of the specimens from ANSYS models are given in Table 4. It can be observed that the displacement ductility is enhanced for group B specimens than that of group A specimens for both the column axial load cases. The ultimate displacement of B1-456 is increased by 21.05% and 48.98% than that of A1-456 during downward and upward loading respectively. Similarly the enhancements in deformation capacity for B2-456 are 46.08% and 3.9% during downward and upward loading.

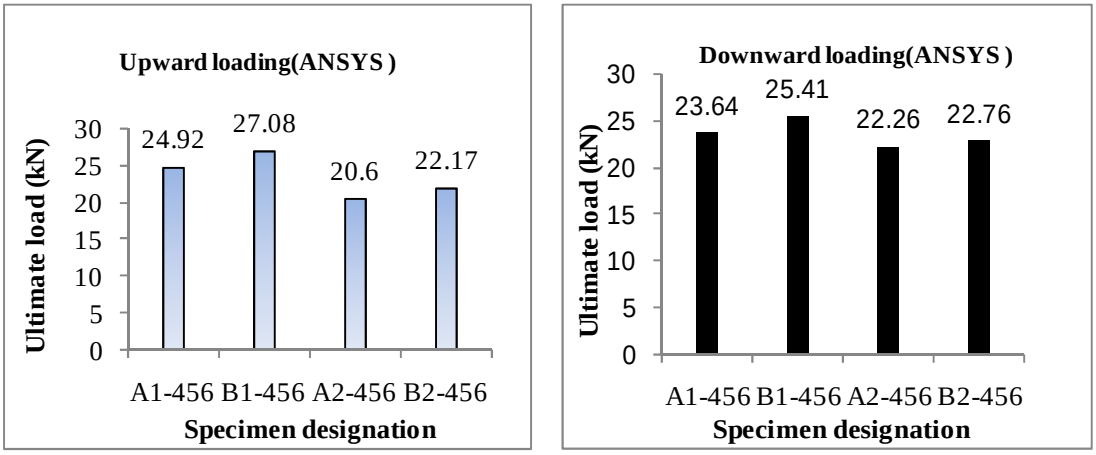

(a) Upward loading (b) Downward loading

Figure 13. Comparison of ultimate load capacities of finite element models.

Table 4. Displacement ductility of specimens from ANSYS model

Specimen	Displacement (mm)				Displacement ductility		Average displace-ment ductility
	Yield		Ultimate				
	Downward direction	Upward direction	Downward direction	Upward direction	Downward direction	Upward direction	
A1-456	5.18	5.87	16.77	27.44	3.24	4.67	3.95
B1-456	4.72	4.59	20.3	40.88	4.3	8.91	6.61
A2-456	4.72	5.02	17.56	17.53	3.72	3.49	3.6
B2-456	4.41	4.59	25.65	18.21	5.82	3.97	4.9

5. CONCLUSIONS

In this paper the performance of exterior beam column joints with non-conventional reinforcement detailing was examined experimentally and numerically. The following conclusions are arrived from this study.

- The test specimens with diagonal confining bars have shown better performance, exhibiting higher strength with minimum cracks in the joint. All the specimens failed by developing tensile cracks at interface between beam and column. The joint region of specimens of group B is free from cracks except some hair line cracks which show the joints had adequate shear resisting capacity.
- The specimens detailed as per IS: 456 with diagonal confining bars had improved ductility and energy absorption capacity than specimens detailed as per IS 456:2000.The displacement ductility is increased considerably for the non-conventionally detailed specimens.
- From the analytical study it is observed that the provision of cross diagonal reinforcement increased the ultimate load carrying capacity and ductility of joints in the both upward and downward loading conditions.

REFERENCES

1. Paulay T. Equilibrium criteria for reinforced concrete beam-column joints, *ACI Structural Journal*, Nov-Dec, **86**(1989) 635-43.
2. Tsonos AG, Tegos IA, Penelis G. Gr. Seismic resistance of type 2 exterior beam-column joints reinforced with inclined bars, *ACI Structural Journal*, **89**(1992) 3-12.
3. Murty CVR, Rai DC, Bajpai KK, Jain SK. Effectiveness of reinforcement details in exterior reinforced concrete beam column joints for earthquake resistance, *ACI*

Structural Journal, **100**(2003) 49-155.
4. Jing LI, Pam HJ, Francis TK. New details of HSC beam-column joints for regions of low to moderate seismicity, *13th World Conference on Earthquake Engineering*, Vancouver, Canada, (2004), Paper No. 449.
5. Shyh-Jiann H, Hung-Jen Lee, Ti-Fa Liao, Kuo-Chou Wang, Hsin-Hung Tsai, Role of hoops on shear strength of reinforced concrete beam-column joints, *ACI Structural Journal*, No. 3, **102**(2005) 578-87.
6. Alva GMS, Ana LHCE, Mounir Khalil ED. An experimental study on cyclic behaviour of reinforced concrete connections, *Canadian Journal of Civil Engineering*, **34**(2007) 565-75.
7. Elyasian I, Abdoli N, Ronagh HR. Evaluation of parameters effective in FRP shear strengthening of R C beams using FE method, *Asian Journal of Civil Engineering (Building and Housing)*, No. 3, **7**(2006) 249-57.
8. IS 1893: 2002, Indian Standard Code on Criteria for Earthquake Resistant Design of Structures, (Bureau of Indian Standards), New Delhi, India, 2002.
9. IS 456:2000, Indian Standard Plain and Reinforced Concrete Code of Practice, (Bureau of Indian Standards), New Delhi, India, 2000.
10. SP 34: 1987, Indian Standard Handbook on Concrete Reinforcement and Detailing, (Bureau of Indian Standards), New Delhi, India, 1987.
11. ANSYS10.0, *ANSYS Users manual*, (ANSYS, Inc.), Canonsburg, 1995.
12. ACI Standard 318-1995, Building code requirement for reinforced concrete and commentary, (American Concrete Institute), Detroit, USA, 1995.
13. Desai P, Krishnan S. Equation for the stress-strain curve of concrete, *ACI Structural Journal*, 61(1964) 345-50.